Extended-MHD simulations of shattered pellet injection into an Ohmic JET plasma

O. P. Bardsley[1], T. C. Hender[1], B. C. Lyons[2], N. M. Ferraro[3], S. N. Gerasimov[1],

H. J. Sun[1], P. J. Carvalho[4], G. Szepesi[1] & JET contributors[*]

[1] *United Kingdom Atomic Energy Authority, Culham Centre for Fusion Energy, Culham Science Centre, Abingdon, Oxon OX14 3DB, UK*

[2] *General Atomics, San Diego, CA 92121, USA*

[3] *Princeton Plasma Physics Laboratory, Princeton, NJ 08543-0451, USA*

[4]*Instituto de Plasmas e Fusão Nuclear, Instituto Superior Técnico, Universidade Técnica de Lisboa, 1049-001 Lisboa, Portugal*

[*] *See the author list of 'Overview of JET results for optimising ITER operation' by J. Mailloux et al. to be published in Nuclear Fusion Special issue: Overview and Summary Papers from the 28th Fusion Energy Conference (Nice, France, 10-15 May 2021)*

Abstract

Disruptions pose a serious challenge for future tokamak power plants; at the large stored thermal and magnetic energies of ITER and DEMO plasmas, the heat loads and electromagnetic forces during disruptions must be mitigated. With this objective, JET experiments employing impurity shattered pellet injection (SPI) have recently been undertaken [1, 2].

We present numerical models of SPI disruptions in JET using M3D-C^1, an extended-MHD code developed for the study of non-linear transient events in tokamaks. Among its extensions are a neutral gas shielding model for the ablation of frozen pellets within the plasma, and the non-coronal equilibrium model KPRAD for tracking impurity charge states and radiation. With these, plasma cooling both before the thermal quench (when there is little MHD activity) and during it (when instability provokes rapid penetration of impurities and cooling of the plasma core) can be modelled.

Our results concern cooling of the Ohmic JET plasma #95149 by a small shattered neon-deuterium pellet, modelled in M3D-C^1 both with linearised stability analyses of axisymmetric simulations, and with a fully non-linear three-dimensional model. Comparisons are made with experimental measurements of temperature profiles and radiated power during the pre-thermal quench phase, and the timing and nature of thermal quench onset as the pellet impinges on rational surfaces and excites low-n MHD activity. This analysis qualifies the numerical approach, paving the way to simulations of higher-energy JET discharges and predictions for future devices.
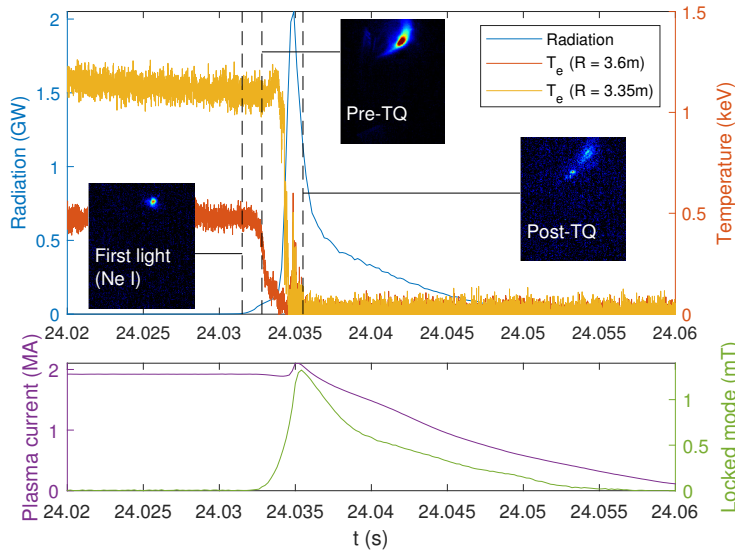
Figure 1: Experiment summary for JET pulse 95149. Images are from KL8-E8WA camera with a 527nm filter, radiation measurements from KB5V bolometer, and midplane electron temperature from KK3F ECE diagnostic.
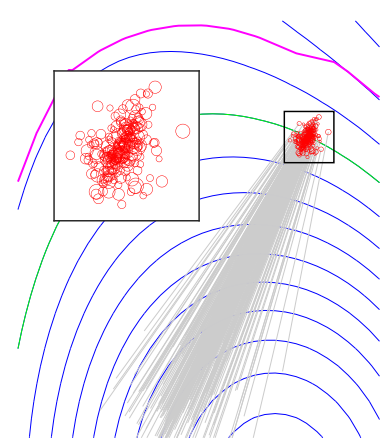

Figure 2: Equilibrium flux surfaces (blue, separatrix in green) and pellet shard cloud used in M3D-C^1 simulations. Shards are red circles, with radius proportional to the physical size. Grey lines show pellet trajectories.

Experimental results

We consider JET shot 95149, a shattered pellet injection (SPI) into a healthy Ohmic L-mode plasma at 2MA/2T. The SPI is neon (0.11g) with a deuterium shell injected from above; the pellet diameter is 4mm, the smallest available, but this is sufficient to instigate a disruption. There is an initial cooling phase (pre-TQ) of 2.5ms, before a rapid (0.5ms) thermal quench (TQ), then a 24ms current quench. A summary of the experiment is shown in Fig. 1.

M3D-C^1 and simulation setup

Numerical simulations are performed using the extended-MHD code M3D-C^1 [3], initialised from a pressure-constrained EFIT equilibrium reconstruction just before the disruption. Neon is added as a plume of 241 shards with a distribution of sizes and trajectories (specified *ad hoc* rather than inferred from experiment), and an average speed of 200m/s (see Fig. 2); its rate of ablation into the plasma is determined by a neutral gas shielding model [4] for each shard. Impurity ionisation, radiation and recombination is calculated for each charge state using the KPRAD model [5]. Spitzer resistivity is used, such that as the impurities cool the plasma edge, current is forced to diffuse inwards. We present results from two near-identical simulations — one in 2D, with material being deposited uniformly around an annulus, and one in 3D, with a Gaussian-shaped deposition of toroidal variance 2.4m. Our analysis focusses on the pre-TQ and identifying onset of the TQ due to MHD activity.
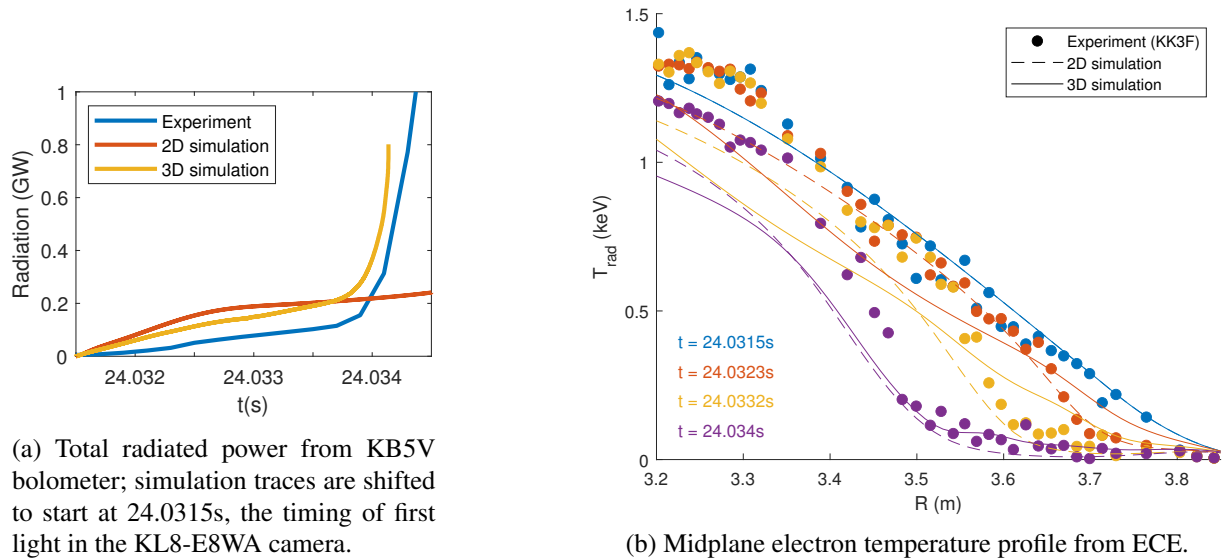
(a) Total radiated power from KB5V bolometer; simulation traces are shifted to start at 24.0315s, the timing of first light in the KL8-E8WA camera.

(b) Midplane electron temperature profile from ECE.

Figure 3: Comparison of the pre-TQ phase between simulations and experiment.

Comparison of pre-TQ

During the pre-TQ, radiation increases with the quantity and temperature of ablated impurities as they penetrate. Measurement of total radiation from the KB5V bolometer, which is offset $90°$ toroidally from the SPI, is compared with simulations in Fig. 3a. The total is the right order of magnitude, despite only $\sim 4\%$ of the neon being ablated in the simulations. The rapid growth indicative of TQ onset is well-captured in the 3D simulation (timing is relative to the observed first light at 24.0315s, not fitted to the data). This suggests the simulation may be capturing the correct MHD trigger, despite the fact it does not progress through the TQ. The two simulations agree well during the pre-TQ phase, with 3D effects responsible for the TQ radiation spike.

More detailed analysis of the pre-TQ phase is possible by looking at the electron temperature profile evolution from ECE (Fig. 3b). (Though note these measurements may not be entirely local during the disruption.) Agreement with simulations is reasonable — despite excessive central cooling caused by higher diffusivities in the simulation, the front moves towards the core at the correct rate in both 2D and 3D cases. The agreement is better in 2D — the 3D cooling pattern may not be accurately reproduced due to the pellet being too wide and the ratio of thermal conductivities too small.

Onset of MHD activity

In the 3D simulation, we observe progressive destabilisation of 2/1 and 3/2 MHD modes, with the latter heralding TQ onset (Fig. 4). Linearised stability analyses of snapshots from the 2D simulation can predict the timing of instability onset and yield consistent growth rates and mode shapes for $n = 1$ and 2, suggesting axisymmetric current contraction is important in MHD
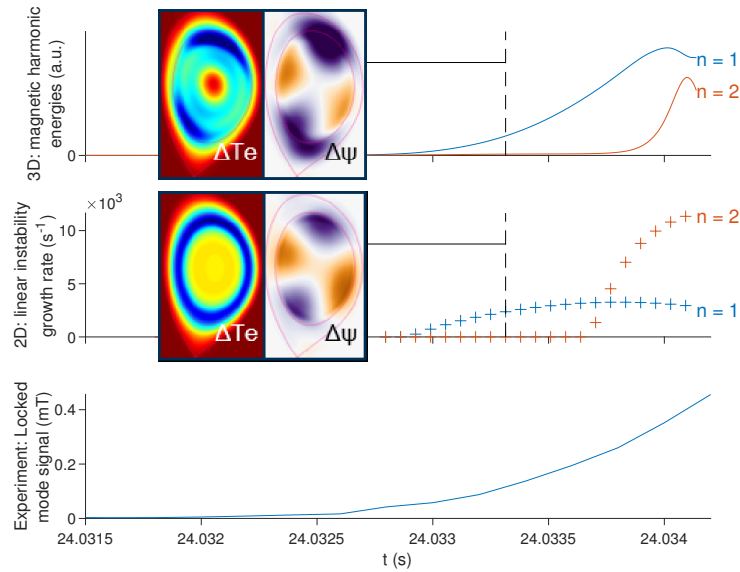
Figure 4: Onset of MHD activity in 3D simulation (top), 2D simulation (middle), and experiment (bottom). Inset are change in electron temperature in both simulations, change in flux function in 3D, and eigenmode in 2D.

destabilisation of the 3D case. However, a radiatively cooled 2/1 island is also observed in 3D, the growth of which may contribute to TQ onset. The timing of $n = 1$ MHD activity is also consistent with experiment.

Conclusions

Simulations of SPI into an Ohmic JET plasma using the extended-MHD code M3D-C[1], in both 2D and 3D, show a pre-TQ evolution of radiation and temperature profile consistent with experiment, despite only a very small quantity of neon ablating into the plasma. The timing of MHD instability, indicated by an upturn in radiation and $n > 0$ magnetic energy, is also well-captured. Linear analyses of the 2D simulation predict instability compatible with the 3D results, although helical island cooling is also significant in 3D.

References

[1] L. R. Baylor et al., FEC 2020, TECH/1-4Rb

[2] S.N. Gerasimov et al., this conference, P1.1031 (2021)

[3] J. Breslau et al., *Phys. Plasmas* **16**, 092503 (2009)

[4] P. B. Parks et al., *Nucl. Fusion* **34**, 417–426 (1994)

[5] B. C. Lyons et al., *Plasma Phys. Control. Fusion* **61**, 064001 (2019)

Acknowledgements